

Investigation of Femtosecond Electronic Dephasing in CdSe Nanocrystals Using Quantum-Beat-Suppressed Photon Echoes

R. W. Schoenlein,⁽¹⁾ D. M. Mittleman,^{(1),(2)} J. J. Shiang,⁽³⁾ A. P. Alivisatos,^{(1),(3)}
and C. V. Shank^{(1),(2),(3)}

⁽¹⁾*Lawrence Berkeley Laboratory, 1 Cyclotron Road, MS 70-193A Berkeley, California 94720*

⁽²⁾*Department of Physics, University of California, Berkeley, California 94720*

⁽³⁾*Department of Chemistry, University of California, Berkeley, California 94720*

(Received 19 August 1992)

We report the first direct measurements of femtosecond electronic dephasing in CdSe nanocrystals using three-pulse photon echoes and a novel mode-suppression technique. We are able to separate the dynamics of the coherently excited LO phonons from the underlying electron-hole dephasing by suppressing the quantum beats. The homogeneous linewidth of these materials at 15 K results from electronic dephasing in ~ 85 fs, approximately half of which is due to acoustic phonon modes. Contributions from acoustic phonons dominate the homogeneous linewidth at room temperature.

PACS numbers: 78.47.+p, 42.50.Md, 42.65.Re, 73.20.Dx

Semiconductor nanocrystals of a size comparable to or smaller than the bulk exciton exhibit a number of novel properties resulting from the three-dimensional quantum confinement. In such systems, the quasicontinuum of electronic states in the bulk is reduced to a series of discrete electronic transitions. This change in the density of states gives rise to large optical nonlinearities and a blueshift of the excitonic absorption peak. Because of the strong dependence of the band gap on size [1], even highly monodisperse samples are substantially inhomogeneously broadened. In addition, the carrier dynamics of these materials are strongly influenced by size. This is a consequence of the confinement of the electron and hole wave functions and of the influence of surface states and phonon coupling, all of which are size dependent.

The electronic properties of CdSe nanocrystals have been studied previously using a variety of techniques. Resonance Raman measurements have been used to investigate electron-phonon coupling in these materials, and have shown significant coupling to the dominant LO phonon mode at 205 cm^{-1} [2-4]. However, as a consequence of the size quantization, this coupling is considerably reduced relative to electron-LO phonon coupling in bulk CdSe [5]. Photoluminescence excitation experiments have also shown evidence of electron-phonon coupling in the absorption spectra of individual CdSe clusters [6]. Time-resolved luminescence measurements as well as spectral hole burning on time scales of nanoseconds [6,7] and hundreds of femtoseconds [6,8,9] have been used to study carrier relaxation dynamics, including surface trapping and dephasing. Pump-probe experiments have shown clear evidence of spectral hole burning at low temperatures [7] with hole widths of several hundred wave numbers. However, such spectral holes include contributions from both electronic dephasing and phonon broadening. At room temperature these effects have prevented the observation of spectral holes that are narrower than the inhomogeneous distribution. Thus it is not possible to directly measure the various contributions to the homogeneous linewidth using hole-burning techniques.

In this paper we demonstrate the use of photon echo techniques to investigate the various processes which contribute to electronic dephasing in quantum-confined systems. Experimental results show a strong modulation of the optically excited polarization by coherent LO phonons at 205 cm^{-1} . By using a novel three-pulse photon echo technique to suppress the effects of these quantum beats, we are able to clearly distinguish between electronic dephasing due to dynamic processes and linewidth broadening due to phonon line structure.

The laser system [10] consists of a colliding-pulse mode-locked (CPM) laser with two multipass dye amplifiers pumped at 400 Hz by a XeF excimer laser. Microjoule pulses from the first amplifier (50 fs, 620 nm) are used to generate a white-light continuum in a jet of ethylene glycol, and the blue-green (484-507 nm) portion of the continuum is reamplified in the second amplifier. A sequence of gratings and prisms are used to directly compress the amplified continuum, resulting in nearly transform-limited pulses of 15 fs duration.

The $\sim 22\text{ \AA}$ diameter CdSe nanocrystals used in this study are grown in solution using the inverse micelle method and are capped with organic selenols [7]. Following the growth process, the particles are annealed at 170°C , and the crystallinity and size distribution are characterized by x-ray powder diffraction, transmission electron microscopy, and linear optical absorption. The variation in particle diameter ($\sim 10\%$) results in an inhomogeneous half-width of $\sim 1100\text{ cm}^{-1}$. The CdSe nanocrystals are uniformly dispersed in a $300\text{ }\mu\text{m}$ free-standing polymer (PMMA) film. The linear absorption spectrum at room temperature shows a distinct excitonic (highest occupied and lowest unoccupied molecular orbital) absorption peak at $\sim 490\text{ nm}$ (optical density ~ 0.5), which merges with an absorption continuum at shorter wavelengths. The $\sim 23\text{ nm}$ bandwidth of the laser pulse is centered on the excitonic absorption peak (at room temperature) to avoid exciting carriers to the continuum states. In all our experiments the excitation fluence is $\sim 0.1\text{ mJ/cm}^2$ (much less than one photon per nanocrystal).

tal) and the detected echo signals exhibit the expected I^3 dependence on laser intensity. Based on the laser fluence and sample absorption, we estimate that heating of the nanocrystals by the optical pulses is negligible on the time scale of our observations.

Our initial measurements of electronic dephasing in these materials, using two-pulse photon echoes, exhibit decay times (τ_{echo}) ranging from ~ 9 fs at 30 K to ~ 6 fs at 235 K. The extremely rapid decay and the temperature dependence suggest that the polarization response measured by the two-pulse echo is strongly modulated by the vibrational modes of the system. This results in significant deviation from the ideal behavior ($\tau_{\text{echo}} = T_2/4$) for an inhomogeneous two-level system.

The modulation of the polarization is confirmed by three-pulse photon echo experiments in which we detect the integrated echo intensity in the phase-matched direction ($-k_1 + k_2 + k_3$) as a function of the delay between the first and second pulse (t_{12}) or as a function of the delay between the first and third pulse (t_{13}). Since the arrival of the third pulse determines when the echo is formed, it is possible to generate the echo at a specific phase of the quantum beat by adjusting t_{13} . In particular, if the third pulse is delayed by exactly one vibrational period, then the nuclei have returned to their original positions and the quantum-beat modulation of the echo is suppressed. In contrast, if the arrival of the third pulse is out of phase with the vibrational period, then the nuclei are maximally displaced and the echo decay is strongly modulated by the quantum beat.

Our results represent the first demonstration of quantum-beat suppression using femtosecond photon echoes, though it was initially described as a means for suppressing modulations due to superhyperfine splitting in electron-spin-echo experiments [11]. For an inhomogeneously broadened system, with a single harmonic mode at a frequency ω , the stimulated echo signal (at absolute zero) in the $-k_1 + k_2 + k_3$ direction is given by [12,13]

$$S(t_{12}, t_{13}) \sim \exp[-4\Delta^2(1 - \cos\omega t_{12})(1 - \cos\omega t_{13})] \\ \times \exp[-4t_{12}/T_2],$$

where T_2 is the electronic dephasing time and Δ is the electron-phonon coupling parameter (dimensionless nuclear displacement). The modulation of the echo response corresponds to the harmonic displacement of the nuclei, $\delta x \sim \Delta[1 - \cos(\omega t)]$, where $\delta x = 0$ refers to the equilibrium position in the ground state (i.e., prior to excitation). Clearly, the quantum-beat modulation of the echo is strongest for $t_{13} = \pi/\omega$ ($\delta x = \text{max}$) and the modulation is completely suppressed for $t_{13} = 2\pi/\omega$ ($\delta x = 0$).

Figure 1 shows the predicted three-pulse photon echo response ($-k_1 + k_2 + k_3$ direction) in the presence of quantum beats, as a function of the delay between the first and second pulse (t_{12}) and between the first and third pulse (t_{13}). This illustrative calculation includes a dephasing time of 80 fs, as well as the (damped) vibrational dynamics of the 205 cm^{-1} LO phonon mode. The

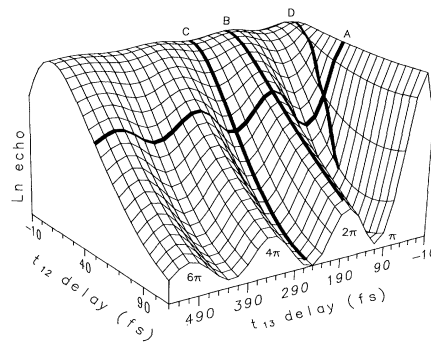


FIG. 1. Calculated three-pulse photon echo signal in the presence of a 200 cm^{-1} phonon mode as a function of delay between pulse one and two (t_{12}) and between pulse one and three (t_{13}). Solid lines *A*, *B*, and *C* correspond to $t_{12} = 50$ fs, $t_{13} = 170$ fs, and $t_{13} = 250$ fs. Solid line *D* corresponds to the two-pulse echo in which $t_{12} = t_{13}$.

solid line *A* represents the expected echo response for a fixed delay of the second pulse ($t_{12} = 50$ fs) as a function of the third pulse delay. The oscillations in *A* result from the vibrational coherence of the LO phonon mode.

The experimental result corresponding to the prediction of Fig. 1, line *A* is shown in Fig. 2. In this measurement of the echo signal as a function of t_{13} (with $t_{12} = 33$ fs), we observe oscillations resulting from the coherent vibrational excitation, and the measured period is consistent with the 205 cm^{-1} LO phonon mode. In addition, we observe that the phonon oscillations are damped on a time scale of 1 ps. This damping is likely due to the decay of optic phonons into acoustic phonons, and is in good agreement with the $\sim 15 \text{ cm}^{-1}$ Raman linewidth measured by Alivisatos *et al.* [2]. These data represent the first time-domain observation of coherent phonons in semiconductor nanocrystals and provide important information about vibrational dynamics in these materials.

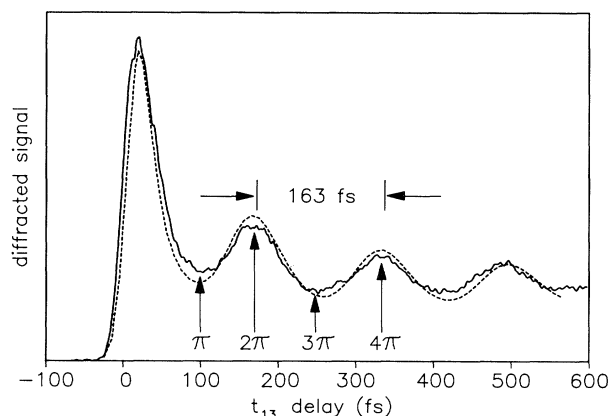


FIG. 2. Three-pulse photon echo (22 \AA particles, 15 K) as a function of t_{13} with $t_{12} = 33$ fs. Dashed line is a theoretical fit with one phonon mode ($\omega = 205 \text{ cm}^{-1}$, $\Delta = 0.7$, $T_{\text{damp}} = 0.7$ ps), and $T_2 = 85$ fs.

In order to directly investigate the electronic dephasing, we can use the results of Fig. 2 to determine the optimal delay for the third pulse. By positioning the third pulse at exactly one LO phonon period ($t_{13}=2\pi/\omega$) and scanning the delay of pulse two (t_{12}) the effects of the vibrational dynamics can be effectively suppressed (Fig. 1, curve *B*). Conversely, if the third pulse is positioned out of phase with the LO phonon ($t_{13}=3\pi/\omega$), then the echo decay will be strongly modulated by the quantum beat (Fig. 1, curve *C*). The corresponding experimental measurements are shown in Fig. 3. With the third pulse in the 2π position ($t_{13}=163$ fs) we measure an echo decay time of ~ 20 fs. With the third pulse in the 3π position ($t_{13}=245$ fs), the echo decay is strongly modulated by the quantum beat, and we measure a much faster echo decay (~ 9 fs). Finally, with the third pulse in the 4π position ($t_{13}=326$ fs), the quantum-beat modulation is again suppressed and the echo decay becomes longer. Note that the optical suppression of the vibrational dynamics is less effective at successively longer delays of the third pulse ($\omega t_{13}=4\pi, 6\pi, 8\pi, \dots$). This is a result of the vibrational damping (Fig. 2) which is an additional contribution to the electronic dephasing that can be suppressed only for $t_{13} \ll T_{\text{damp}}$.

The dashed lines in Figs. 2 and 3 are calculations based on a theoretical model which accounts for both the electronic and vibrational dynamics of the system. The electronic dynamics are described as a two-level system using a standard density-matrix formalism to calculate the third-order polarization response. The vibrational dynamics of the LO phonon mode are described by offset harmonic potentials in the ground and excited states, where Δ is the dimensionless displacement. This description is incorporated into the density matrix using a semi-classical formalism, with a frictional term to account for the vibrational damping [13]. The calculation includes

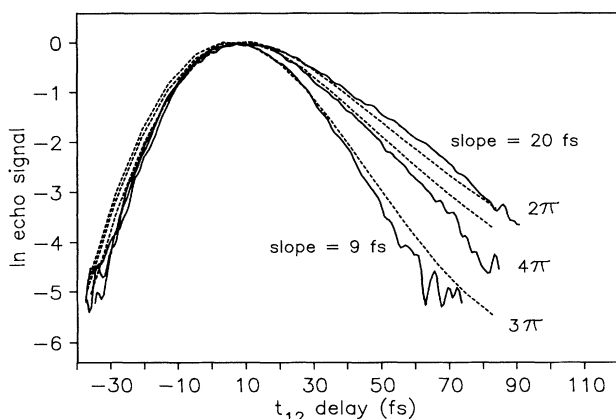


FIG. 3. Three-pulse echo (22 Å particles, 15 K) as a function of t_{12} , with the third pulse in phase ($t_{13}=2\pi/\omega, t_{13}=4\pi/\omega$), and out of phase ($t_{13}=3\pi/\omega$), with the quantum beat (163 fs period). Dashed lines are theoretical fits with one phonon mode ($\omega=205$ cm $^{-1}$, $\Delta=0.7$, $T_{\text{damp}}=0.7$ ps), and $T_2=85$ fs.

one damped vibrational mode ($\omega=205$ cm $^{-1}$, $\Delta=0.7$, $T_{\text{damp}}=0.7$ ps), consistent with Raman measurements [2], as well as realistic laser pulse parameters and finite inhomogeneous broadening. We also assume an electronic dephasing time T_2 of 85 fs and a lifetime (T_1) scaling to describe the partial recovery (~ 150 fs time constant) of the absorption saturation which we observe in pump-probe measurements. With these parameters we obtain remarkably good fits to the data shown in Fig. 2, including the period, amplitude, and vibrational damping of the oscillations. The same parameters also give a good fit to the results in Fig. 3 including the variation of the echo decay times for $\omega t_{13}=2\pi, 3\pi$, and 4π . Note that the ~ 20 fs echo decay for the $t_{13}=2\pi/\omega$ data in Fig. 3 is approximately $T_2/4$ ($T_2=85$ fs). The discrepancy is the result of the vibrational damping which contributes a small component to the electronic dephasing even at $t_{13}=2\pi/\omega$, and has an increasing effect for longer third pulse delays.

These results provide a good picture of the dynamic evolution of electron-hole coherence in the CdSe nanocrystals. We have identified two processes which modulate the polarization in very different ways. First, the measurements of Fig. 3 indicate a polarization dephasing time (T_2) of ~ 85 fs. Second, significant electronic coupling to the LO phonon mode at 205 cm $^{-1}$ results in a periodic modulation of the polarization. This damped quantum beat is clearly observed in the three-pulse echo data of Fig. 2. The rapid echo decay observed in the two-pulse echo measurements ($t_{12}=t_{13}$, curve *D* in Fig. 1) results from the simultaneous effects of both processes.

We can obtain some insight into the nature of the fundamental polarization dephasing by suppressing the quantum-beat modulation, and investigating the temperature dependence of the echo decay. As shown in Fig. 4, the decay rate scales roughly linearly with temperature from ~ 0.047 fs $^{-1}$ at 15 K to ~ 0.16 fs $^{-1}$ at 240 K. This rather strong temperature dependence cannot be accounted for by the increasing LO phonon population. This fact is illustrated by the dashed line in Fig. 4, which shows the temperature dependence predicted by the same model and parameters used in Figs. 2 and 3. The weak temperature dependence predicted by this model is easily understood, since the effects of the LO phonon mode have been largely suppressed by the position of the third pulse. In addition, since the phonon energy is 25 meV, thermal population of higher vibrational levels in the ground state is not significant in this temperature range.

The linear temperature dependence shown in Fig. 4 strongly suggests that this component of the dephasing rate is the result of coupling to low-frequency acoustic phonons. Such coupling is significantly enhanced in nanocrystals relative to bulk CdSe due to the quantum confinement [5,14]. The numerous compression and expansion modes of each nanocrystal effectively modulate the band gap thereby contributing to the polarization dephasing. By approximating the quasicontinuum of acoustic modes by a single mode (following [7]), we can accu-

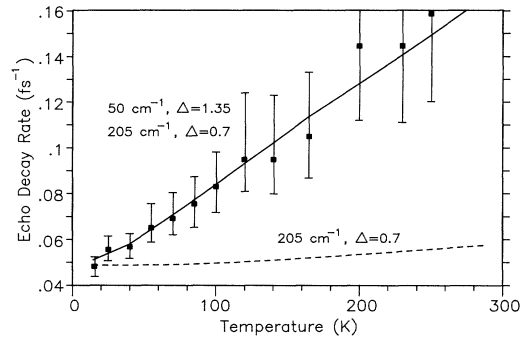


FIG. 4. Temperature dependence of the echo decay rate (22 Å particles) with $t_{13}=2\pi/\omega$ for suppression of the quantum beat. Dashed line is the temperature dependence predicted using the fit parameters from Figs. 2 and 3. Solid line is a theoretical fit using the parameters from Figs. 2 and 3 with one additional mode (50 cm^{-1} , $\Delta=1.35$) to approximate the coupling to the continuum of acoustic phonons.

rately predict the temperature dependence of the dephasing (Fig. 4, solid line) using the theoretical model described previously. Typical parameters of $\hbar\omega=50\text{ cm}^{-1}$ and $\Delta=1.35$ have been used although comparable fits are obtained by using $\hbar\omega=25\text{ cm}^{-1}$ with $\Delta=3.5$, or $\hbar\omega=75\text{ cm}^{-1}$ with $\Delta=0.85$. The particular values of these parameters are not significant, because they are an approximate description of a “heat bath” (i.e., a distribution of modes and coupling parameters). In addition to the linear temperature dependence of the echo decay rate, there is also an offset ($\sim 0.024\text{ fs}^{-1}$) corresponding to a temperature-independent component of the dephasing. Thus the polarization dephasing rate, $(4\tau_{\text{echo}})^{-1}$, may be described by $(T_2)^{-1}=(\tau_{\text{acoustic}})^{-1}+(\tau_0)^{-1}$, where τ_{acoustic} has a linear temperature dependence (for $k_B T > \hbar\omega$) and represents the component of the electronic dephasing resulting from acoustic phonon coupling. τ_0 represents the temperature independent contribution to the electronic dephasing which may result from surface trapping or other defect scattering processes. This component ($\tau_0 \approx 170\text{ fs}$) is entirely consistent with the time constant of the partial recovery (change of state) which we observe in pump-probe measurements. The temperature dependence of the echo decay suggests that coupling to acoustic phonons is a major contributor to the electronic dephasing at room temperature. Even at low temperatures, coupling to acoustic phonons accounts for roughly half of the dephasing rate ($\tau_0 \approx \tau_{\text{acoustic}}$ at 15 K). Our results do not discount the possibility that processes such as phonon-assisted surface trapping [15] may contribute to the temperature dependence of the dephasing.

In summary, using three-pulse photon echo techniques, we have observed in 22 Å CdSe nanocrystals a coherent phonon mode at 205 cm^{-1} which is damped on a picosecond time scale. This vibrational mode gives rise to quantum beats which strongly modulate the electron-hole polarization and mask the underlying dephasing dynamics. The effects of this quantum beat are suppressed by

appropriate positioning of the third pulse, enabling us to directly probe the fundamental dephasing processes. Our results indicate that the polarization dephasing occurs on a time scale of $\sim 85\text{ fs}$ at 15 K, and is roughly linearly dependent on temperature, with a dephasing time of only $\sim 25\text{ fs}$ at 240 K. The temperature dependence of the dephasing is consistent with enhanced coupling to a multitude of acoustic modes which is expected to occur in such quantum-confined systems [5,14]. This interpretation leads to the conclusion that nearly all of the dephasing (i.e., nearly all of the homogeneous linewidth) in CdSe nanocrystals at room temperature is the result of acoustic phonon coupling. Even at low temperatures (15 K), acoustic phonon coupling accounts for roughly half of the homogeneous linewidth. The remainder of the dephasing ($\sim 170\text{ fs}$) may be due to surface trapping, defect scattering, or other processes. Additional studies on particles of different sizes and surface passivations should allow us to determine the nature of this temperature-independent contribution to the dephasing.

We wish to acknowledge assistance from W. T. Pollard in generating the code for the numerical simulations, and helpful discussions with C. J. Bardeen. This work was supported by the U.S. Department of Energy under Contract No. DE-AC0376SF00098.

- [1] L. Brus, *J. Chem. Phys.* **80**, 4403 (1984).
- [2] A. P. Alivisatos, T. D. Harris, P. J. Carroll, M. L. Steigerwald, and L. E. Brus, *J. Chem. Phys.* **90**, 3463 (1989).
- [3] M. C. Klein, F. Hache, D. Ricard, and C. Flytzanis, *Phys. Rev. B* **42**, 11123 (1990).
- [4] A. Tanaka, S. Onari, and T. Arai, *Phys. Rev. B* **45**, 6587 (1992).
- [5] S. Schmitt-Rink, D. A. B. Miller, and D. S. Chemla, *Phys. Rev. B* **35**, 8113 (1987).
- [6] M. G. Bawendi, W. L. Wilson, L. Rothberg, P. J. Carroll, T. M. Jedju, M. L. Steigerwald, and L. E. Brus, *Phys. Rev. Lett.* **65**, 1623 (1990).
- [7] A. P. Alivisatos, A. L. Harris, N. J. Levinos, M. L. Steigerwald, and L. E. Brus, *J. Chem. Phys.* **89**, 4001 (1988).
- [8] P. Roussignol, D. Ricard, C. Flytzanis, and N. Neuroth, *Phys. Rev. Lett.* **62**, 312 (1989).
- [9] N. Peyghambarian, B. Fluegel, D. Hulin, A. Migus, M. Joffre, A. Antonetti, S. W. Koch, and M. Lindberg, *IEEE J. Quantum Electron.* **25**, 2516 (1989).
- [10] R. W. Schoenlein, J.-Y. Bigot, M. T. Portella, and C. V. Shank, *Appl. Phys. Lett.* **58**, 801 (1990).
- [11] W. B. Mims, *Phys. Rev. B* **6**, 3543 (1972); W. B. Mims, *Phys. Rev. B* **5**, 2419 (1972).
- [12] E. J. Heller, *J. Chem. Phys.* **62**, 1544 (1975).
- [13] Y. J. Yan and S. Mukamel, *J. Chem. Phys.* **89**, 5160 (1988); Y. J. Yan and S. Mukamel, *J. Chem. Phys.* **94**, 179 (1991).
- [14] S. Nomura and T. Kobayashi, *Phys. Rev. B* **45**, 1305 (1992).
- [15] M. G. Bawendi, P. J. Carroll, W. L. Wilson, and L. E. Brus, *J. Chem. Phys.* **96**, 946 (1992).